Chemical Engineering Journal 145 (2009) 461–467

Contents lists available at ScienceDirect

Chemical Engineering Journal

journal homepage: www.elsevier.com/locate/cej

The comparison between the polyol process and the impregnation method for the preparation of CNT-supported nanoscale Cu catalyst

Chi-Yuan Lu [a], Hui-Hsin Tseng [b], Ming-Yen Wey [c,*], Ting-Wei Hsueh [c]

[a] Department of Public Health, Chung Shan Medical University, Taichung 402, Taiwan, ROC
[b] Department of Occupational Safety & Health and Graduate Program, Chung Shan Medical University, Taichung 402, Taiwan, ROC
[c] Department of Environmental Engineering, National Chung-Hsing University, Taichung 402, Taiwan, ROC

ARTICLE INFO

Article history:
Received 17 November 2007
Received in revised form 29 March 2008
Accepted 24 April 2008

Keywords:
Carbon nanotube
Catalyst
Polyol process
Impregnation
Oxidation

ABSTRACT

Carbon nanotubes (CNTs) are relatively potential materials for catalyst supports. CNT-supported Cu catalysts were prepared by an impregnation method and a polyol process. The catalytic activity was examined under different reaction atmospheres, Cu contents, and sizes of supports for CO oxidation. The experimental results showed that the active phase on the catalyst prepared by the impregnation method (10–20 nm) was smaller than that on the catalyst prepared by the polyol process (30–50 nm). Furthermore, the smaller active phase showed better performance for CO oxidation. Therefore, catalysts prepared by the impregnation method had a lower activation energy (57.47 kJ mol^{-1}) than those prepared by the polyol process. The optimum CNT-supported Cu catalyst prepared by the impregnation method using 10–20 nm CNTs had a Cu content of 13.4 wt.%, and a CO conversion of 33% achieved at 125 °C with a total space velocity of 1.56×10^5 h^{-1}.

1. Introduction

The principal factor that causes air pollution is the incomplete combustion of petroleum fuels, which discharges pollutants such as hydrocarbons and carbon monoxide (CO) into the air. Among all the air pollutants, carbon monoxide is by far the most abundant and harmful pollutant affecting both the human body and the environment. Currently, the catalytic oxidation of CO to carbon dioxide (CO_2) is known as the most effective post-treatment for reducing CO emissions.

Many researchers have conducted CO oxidation using various metals (Pt, Au, Cu, Ce, Co) as catalysts and found that the type, dispersion, and particle size of metals on the support material have significant impact on catalytic activity [1–5]. Numerous metal-supported catalysts investigated to date showed that the support is also an important factor that influences the catalytic activity in the reaction. Various material supports such as activated carbon (AC), alumina, silica, clay, zeolite and carbon nanotubes (CNTs) [1–11] have been studied. The characteristics of a good support material include large specific surface area, unique pore structure, large adsorption capacity, good mechanical strength, high chemical and thermal stability, and hydrophobicity. Since CNTs have such characteristics, they have attracted considerable attention as potential supports [9–11].

In previous studies [11], we used CNTs as supports to prepare Co catalysts with impregnation method and compared their activity with AC-supported Co catalysts in CO oxidation. The results indicated that CNTs had better thermal stability and mass transition efficiency than AC, and the active sites could be highly dispersed on CNTs with nanosized particles. Moreover, we studied the polyol process to prepare catalysts for the removal of pollutants [12], and the results indicated that this process can generate well-dispersed metal nanoparticles on the support AC. The polyol process, a method used for monodisperse metal powders, involves a redox reaction between a metallic compound and a liquid polyol [13]. In comparison to earlier studies [11,12], our results indicated that both support (CNT) and preparation (polyol process) could enhance the catalytic activity as a good prepared catalyst. Thus, it is possible to prepare the high activity catalyst by combining CNT support and polyol process. In order to study the effect of polyol process on CNT-supported catalyst preparation, the impregnation method was also employed. Considering the cost of catalyst preparation and activity, Cu with low price and good CO conversion efficiency [4,5] was chosen as active site in this study.

This study mainly focuses on the preparation of CNT-supported Cu catalysts by using polyol process and impregnation method to evaluate the catalytic activity for CO oxidation using different diameters of CNTs and different weights of Cu loading. To throw

* Corresponding author. Tel.: +886 4 22852455; fax: +886 4 22862587.
E-mail address: mywey@dragon.nchu.edu.tw (M.-Y. Wey).

1385-8947/$ – see front matter © 2008 Elsevier B.V. All rights reserved.
doi:10.1016/j.cej.2008.04.033

some light on this matter, the characterization of the catalysts was studied by inductively coupled plasma-mass spectrometer (ICP-MS), field emission scanning electron microscopy (FESEM) with backscattered electrons, transmission electron microscopy (TEM), and X-ray powder diffractometry (XRD).

2. Experimental

2.1. Preparation of catalysts

The CNTs were grown from the Fe nanoparticles produced by chemical vapor deposition (CVD) method at 650 °C with C_2H_2 (H_2:C_2H_2 = 6:1) for 1 h. The CNTs were then soaked in the acid solution (H_2SO_4:HNO_3 = 1:3) for 24 h to remove the Fe particles, followed by the steps of washing, filtering and drying at 110 °C for 24 h. Finally, the Cu/CNT catalysts were prepared by the polyol process and impregnation method.

In this experiment, the nominal Cu loading weight on the CNT was 10 wt.%. Cu/CNT-I catalyst was prepared with excess-solution impregnation using $Cu(NO_3)_2{\cdot}2.5H_2O$ as precursor. During the impregnation, the solutions (9.0 g CNT and 3.66 g $Cu(NO_3)_2{\cdot}2.5H_2O$ were dissolved in the distilled water) were heated at 70 °C and constantly stirred until totally evaporated. Cu/CNT-P catalyst was prepared with polyol process as follows: A given amount of CNT was added to an ethylene glycol–PVP–copper precursor solution, and mixed with a magnetic stirrer. Then, the suspension was heated to a given temperature. At the end of the reaction time, the preparation was rapidly cooled to room temperature with ice-water bath. The catalyst was obtained by filtration and repeated washing of ethanol in order to remove the organic phase. Afterwards, the CNT-supported Cu catalysts, Cu/CNT-I and Cu-CNT-P were dried at 110 °C for 2 h and calcined at 500 °C for 4h in the presence of hydrogen (5% H_2 and 95% He) to get the catalysts.

2.2. Characterization of catalysts

The loading weight of Copper on CNT was determined by inductively coupled plasma-mass spectrometer (ICP-MS, PerkinElmer, SCIEX ELAN 5000). Particle size, powder morphologies and elemental structure of the loadings were investigated using field emission scanning electron microscopy (FESEM; Model JSM-6700F, JEOL, Tokyo, Japan) operated at 5 kV accelerating voltage and equipped with backscattered electrons.

Transmission electron microscopy (TEM) observations were made with a Philips 400T microscope operated at 120 keV to observe the dispersion of active site on the support surface. The samples were suspended in ethanol. After ultrasonic dispersion, a droplet was deposited on a copper grid supporting a perforated carbon film.

An X-ray powder diffractometry (XRD) (SIEMENS D5000) was used to identify the crystalline species of CNT-supported Cu catalysts. A Cu tube with a working voltage of 30 V and a current of 20 A was employed as an X-ray source to estimate the active site phase. The powdered samples were pressed onto suitable holders. The scanning range of 2θ was from 20° to 80° with a scanning speed of 4° min^{-1}. Diffraction patterns were manually analyzed with the Joint Committee of Powder Diffraction Standard (JCPDS) card.

2.3. Activity test

Catalytic activity measurements for the CO oxidation were conducted at atmospheric pressure in a micro-catalytic reactor of 9 mm ID quartz tube under a steady-state condition. The catalysts were placed on quartz filter board. Sample weight of ca. 0.2 mg and flow rates of 400 ml min^{-1} of the feed gas ($CO/N_2/O_2$) governed by Brooks mass flow controller were used for the activity test. The concentrations of CO, CO_2, and O_2 at inlet and outlet of the reactor were both monitored by an online flue gas analyzer (Horiba, PG-250). Before we carried out the experiments, we tested the stability of the system by repeating it three times in order to improve the accuracy of the measured data.

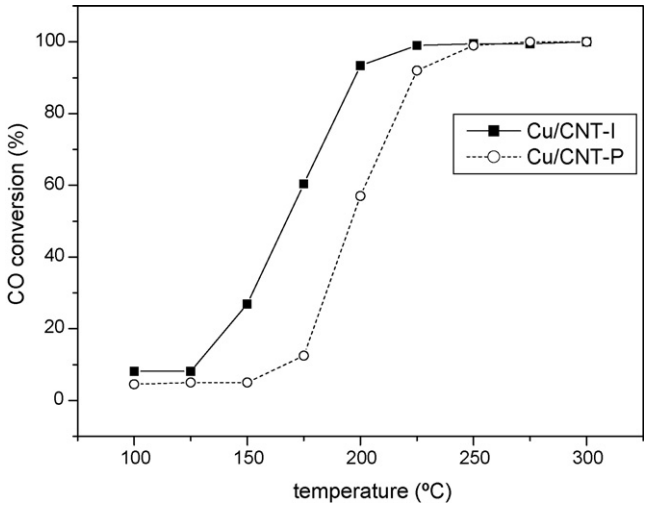

Fig. 1. CO conversion over CNT-supported 7.5 wt.% Cu catalysts as a function of the reaction temperature by different catalyst preparation method (feed composition: 400 ppm CO, SV = 1.56×10^5 h^{-1}, and 6% O_2 in N_2).

3. Results and discussion

3.1. Comparison between the polyol process and the impregnation method

Fig. 1 shows the CO conversion over the Cu/CNT-I and Cu/CNT-P catalysts with 10 wt.% nominal Cu content as a function of the reaction temperature. The inlet feed stream contained 400 ppm of CO and 6% O_2 in N_2 with a total space velocity of 1.56×10^5 h^{-1}. Under the reaction temperature of 100–300 °C, we observed that the activity of Cu/CNT-I is better than that of Cu/CNT-P. At 150 °C, the performance of the CO conversion for Cu/CNT-I is 26.9%, whereas there is no activity for Cu/CNT-P. At temperature up to 175 °C, the Cu/CNT-P catalyst shows 12.5% CO conversion. Although both Cu/CNT-I and Cu/CNT-P catalysts exhibited same reaction tendency with increasing temperature, Cu/CNT-I shows better performance on CO conversion at temperature between 150 and 200 °C. In order to understand the reason for the high activity of Cu/CNT-I, the catalysts were analyzed with ICP-MS to determine the actual Cu loading weight. The results indicated that the actual Cu contents on Cu/CNT-I and Cu/CNT-P were 7.5 and 7.2 wt.%, respectively. This shows that the Cu loading weights on the catalysts prepared by different methods were similar when CNTs were chosen as supports. Since Cu/CNT-I and Cu/CNT-P had the same amount of active phase, the difference in catalytic activity must be due to other factors such as size, shape, crystal structure, and dispersion of the active phase.

Fig. 2(a and d) shows the FESEM images of the CNT-supported Cu catalysts prepared by the impregnation method and polyol process. Although the active phase is spherical in both Cu/CNT-I and Cu/CNT-P, the size of the Cu particles of Cu/CNT-I is smaller than that of the Cu particles on Cu/CNT-P. As a result, Cu/CNT-I shows a better dispersion of Cu particles. The size of the Cu particles on Cu/CNT-I is 10–20 nm, whereas that of the Cu particles on Cu/CNT-P is 30–50 nm. In order to determine the crystal structure of the active phase on CNT-supported Cu catalysts, their XRPD patterns were

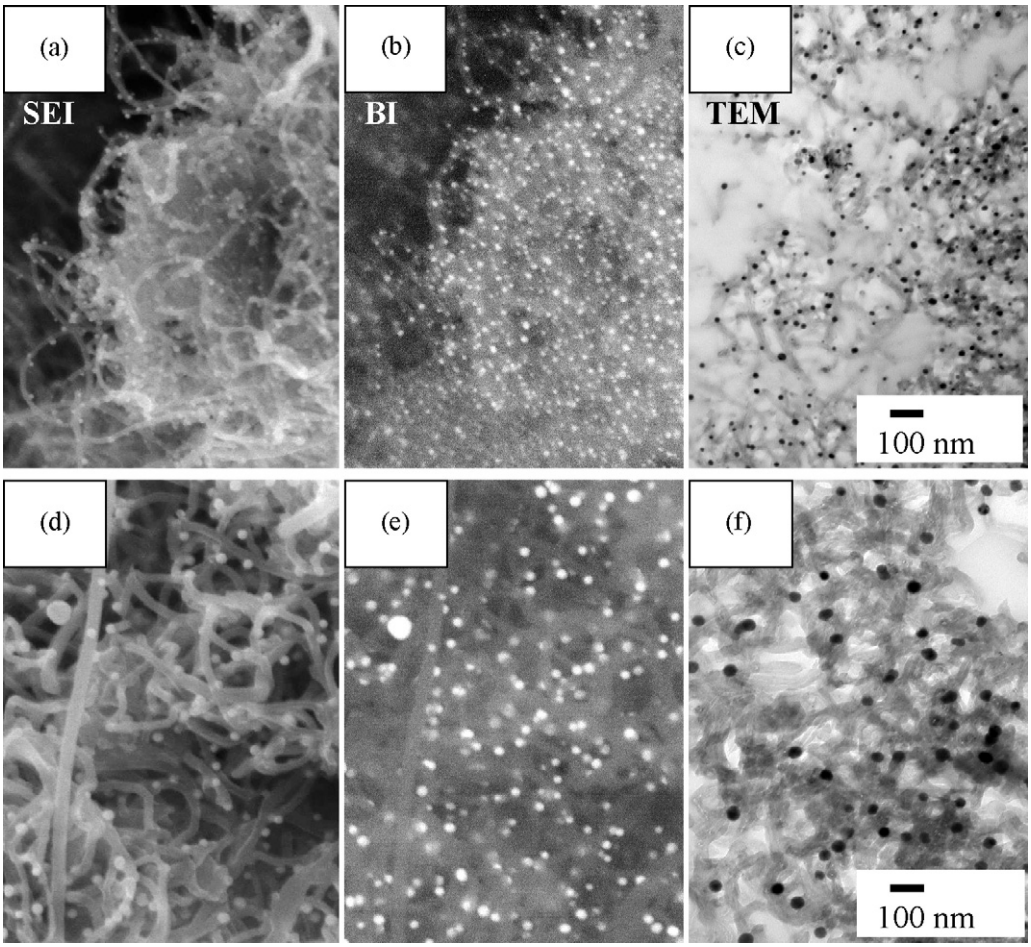

Fig. 2. FESEM-SEI, FESEM-BEI, and TEM-cross-sectional area images of CNT-supported 7.5 wt.% Cu catalysts with different preparation: (a–c) for impregnation method; (d–f) for polyol process.

measured. Fig. 3 shows the XRPD patterns of the CNTs, Cu/CNT-I, and Cu/CNT-P with 2θ scanning from 20° to 80°.

The peak at $2\theta = 27.2°$ can be attributed to the typical graphite structure (0 0 2) of the CNT support. After Cu was loaded on the CNT, additional peaks appeared at $2\theta = 37.6°, 41.7°, 43.3°, 57.2°, 67.8°$, and 77.1°, which were attributed to the major zero-valent copper phase (Cu(1 1 1)), whereas the intensity of Cu_2O, CuO, and Cu_4O_3 were all lower than that of Cu. Therefore, Cu metal was the major active site for the reaction, followed by Cu_2O, CuO, and Cu4O_3. By comparing the intensities of patterns between Cu/CNT-I and Cu/CNT-P, the intensity of Cu/CNT-P was found to be stronger than that of Cu/CNT-I. This revealed that the bigger the Cu particles (30–50 nm) supported on Cu/CNT-P (as shown in Fig. 2), the stronger the XRPD patterns. Furthermore, the mean Cu particle size D can be determined from the Cu(1 1 1) peaks by Scherrer equation. The mean Cu particle size of catalyst for Cu/CNT-I and Cu/CNT-P is 19.2 and 30.7 nm, respectively. When comparing the calculated sizes of Cu active phases with the measured size from the SEM images (Fig. 2), the Cu particle sizes were almost the same size as in the experiment.

In this study, the actual Cu loading weight on the CNT was 7.5 wt.%. Therefore, the high loading weight of the metal leads to the high intensity of the XRPD patterns. On the other hand, because the dispersion of the active phase cannot be determined by XRD analysis, this study employed FESEM and TEM images to determine the dispersion quality of Cu particles. To observe the dispersion of the active phase clearly, the backscattered electrons were used to form an electron backscatter diffraction (EBSD) image with the

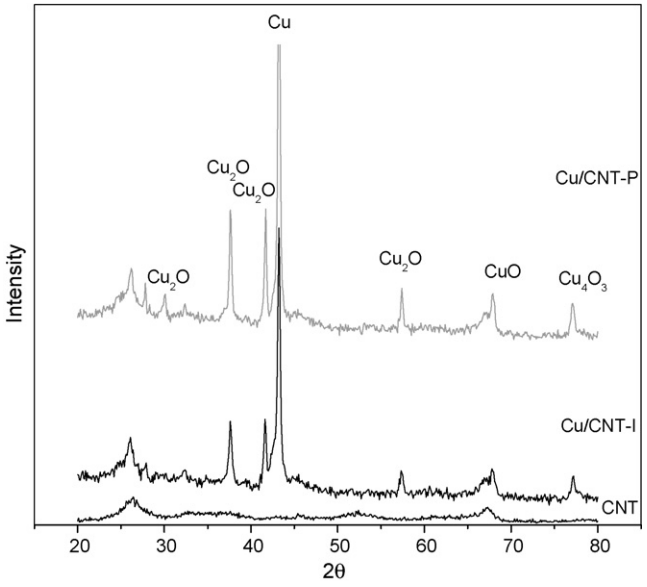

Fig. 3. Measured XRPD patterns of the CNT-supported 7.5 wt.% catalysts with different preparation method.

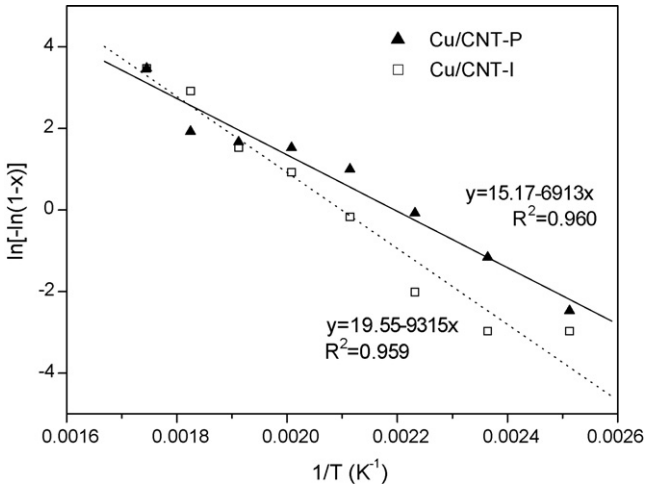

Fig. 4. Arrhenius plots for CO oxidation at (100–300 °C) over Cu/CNT-I and Cu/CNT-P.

FESEM analysis. Backscattered electrons are high-energy electrons that rebound from the sample surface [14]. The quantity of electrons backscattered from a given surface is proportional to the mean atomic number (Z) of the sample material. As a result, a material with a high mean Z will produce more backscattered electrons than a material with a low mean Z. Fig. 2 shows the FESEM images of Cu/CNT-I and Cu/CNT-P, including the scanning electron images (SEI) and backscattered electron images (BEI). Since the catalyst comprises carbon and copper, as shown by the XRPD patterns (Fig. 3), it is observed that the light area corresponds to copper, whereas the dark area mostly corresponds to carbon as shown in Fig. 2(b and e). Therefore, the dispersion of the Cu particles can be clearly observed. Fig. 2(b and e) shows that the size of the Cu particles on Cu/CNT-I at high dispersion is smaller than that of the Cu particles on Cu/CNT-P. In addition, the cross-sectional TEM images of Cu/CNT-I and Cu/CNT-P catalysts have been analyzed using the microtome technique, as shown in Fig. 2(c and f). According to the analysis, the shape of carbon nanotubes could not be observed clearly as opposed to the shape of Cu particles which could be seen clearly. This proved that the dispersion and particle size of Cu on the Cu/CNT-I were better and smaller than that of the Cu particles on Cu/CNT-P.

In order to calculate the activation energy, the reaction order of carbon monoxide and oxygen were both measured at 175 °C. For CO test, the feed contained 0.05% to 2% CO and 12% O_2 in N_2; for O_2 test, the feed contained 0.5% CO and 1% to 6% O_2 in N_2. The experiment results indicated that the reaction orders for CO and O_2 are first and zero, respectively. Thus, the overall CO oxidation over Cu/CNT catalyst is a first-order reaction, and the Eq. (1) was used to calculate the activation energy of the CO conversion [15,16]:

$$\ln[-\ln(1-x)] = \ln A + \ln\left(\frac{v}{u}\right) - \left(\frac{E_a}{RT}\right) \quad (1)$$

where u is the flow rate in ml s^{-1}; v is the total volume of the catalyst in ml; A is the pre-exponential factor in s^{-1}; E_a, the apparent activation energy in kJ mol^{-1}; R, the gas constant is 8.314 J mol^{-1} K^{-1}; T, the absolute temperature in K; and x, the CO to CO_2 conversion rate.

As shown in Fig. 4, the value of the activation energy can be read from the slope by plotting $\ln[-\ln(1-x)]$ against $1/T$. The pre-exponential factor A can be calculated from the intercept. For Cu/CNT-I and Cu/CNT-P, the activation energies are 57.47 and 77.45 kJ mol^{-1}, respectively. We observed that Cu/CNT-I has a lower activation energy than Cu/CNT-P. This reconfirms that the CO conversion increases when nano-copper particles are small and when dispersion on Cu/CNT-I is excellent.

From the above discussion, it is evident that impregnation is a simple and cheap method to prepare a good catalyst under specific conditions, where a nanoscaled material such as CNT was chosen as a support for catalyst preparation. CNTs can enhance the diffusion of active sites in the catalyst preparation process, producing good dispersion and nanoscaled Cu particles on the catalyst, whereas the polyol process showed no notable modification in the preparation of CNT-supported catalyst. In the following experiment, impregnation method was chosen to prepare different CNT-supported catalysts under different operating conditions.

3.2. Effect of oxygen

In this step, we chose the high-activity Cu/CNT-I catalyst to study the effect of oxygen on CO oxidation. The inlet feed stream comprised 400 ppm CO in N_2 at a space velocity of 1.56×10^5 h^{-1} with 0% and 6% O_2. Fig. 5(a and b) shows the CO conversion and CO_2 selectivity over Cu/CNT-I for different reaction atmospheres. The CO_2 selectivity is defined as the ratio of CO_2 formation from CO.

In the absence of O_2, as shown in Fig. 5(a), the CO conversion was carried out when the reaction temperature was above 200 °C. The Boudouard reaction occurred for CO conversion when:

$$2CO \rightarrow C + CO_2 \quad (2)$$

As show in Fig. 5, CO oxidation commenced at 150 °C in the presence of O_2. Two possible reaction mechanisms are involved in CO oxidation. In the first mechanism according to the Mars–Van

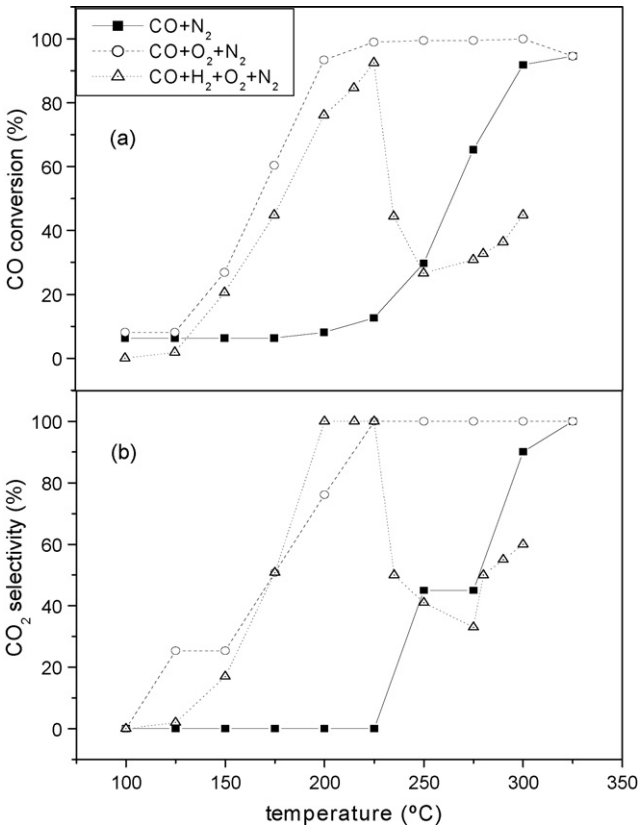

Fig. 5. (a) CO conversion and (b) CO_2 selectivity over Cu/CNT-I in the different reaction atmosphere: (■) in the absence of O_2 (feed composition: 400 ppm CO in N_2), (○) in the presence of O_2 (feed composition: 400 ppm CO and 6% O_2 in N_2), and (△) in the H_2-rich atmosphere (feed composition: 77% H_2, 5000 ppm CO, and 0.5% O_2 in N_2).

Krevelen model [17], the reaction occurs as follows:

$$Cu + \tfrac{1}{2}O_2 \rightarrow CuO \quad (3)$$

$$CuO + CO \rightarrow Cu + CO_2 \quad (4)$$

In the first step (reaction (3)), Cu reacts with O_2 to form an oxidized catalyst; subsequently, CO reacts with the oxidized catalyst to form CO_2, which is later replenished by a reaction with O_2 to form a redox cycle reaction.

In the second conversion mechanism [18], CO is adsorbed on the CNT supported Cu catalyst, while O_2 is cleaved to form O–O bonds. CO then quickly reacts with an O atom to form CO_2:

$$CO_{(gas)} \rightarrow Cu\text{–}CO_{(ads)} \quad (5)$$

$$O_2 \rightarrow 2O_{(ads)} \quad (6)$$

$$Cu\text{–}CO_{(ads)} + O_{(ads)} \rightarrow Cu\text{–}CO_{2(ads)} \quad (7)$$

$$CO_{2(ads)} \rightarrow CO_{2(gas)} \quad (8)$$

From the above discussion, it is evident that CO may completely convert to CO_2 under ideal conditions, confirmed by the CO_2 selectivity shown in Fig. 5. Furthermore, this experiment also investigated the effect of hydrogen by conducting the CO conversion in a H_2-rich atmosphere. Fig. 5(a and b) shows the evolution of CO conversions and CO_2 selectivity obtained over Cu/CNT-I as a function of temperature. The feed contained 5000 ppm CO, 0.5% O_2, and 77% H_2 in N_2 with a space velocity of $1.56 \times 10^5\ h^{-1}$. The experimental observations of the CO conversion in the H_2-rich atmosphere can be separated into three reaction zones on the basis of temperature. First, when the CO conversion increases with temperature, a maximum CO conversion of 93% is achieved at 225 °C. The CO_2 selectivity also shows a similar trend when the temperature was set between 100 and 225 °C. In this step, the CO conversion is not affected by H_2. Finally, the CO conversion and CO_2 selectivity are decreased at reaction temperatures above 225 °C, resulting the CO conversion to decrease to a minimum of 26% at 250 °C. In the previous study [8,11], in addition to the main reaction ($CO + O_2 \rightarrow CO_2$), the following side reactions also occurred:

$$H_2 + \tfrac{1}{2}O_2 \rightarrow H_2O \quad (9)$$

$$CO_2 + H_2 \rightarrow CO + H_2O \quad (10)$$

$$CO + 3H_2 \rightarrow CH_4 + H_2O \quad (11)$$

In the excess H_2-rich atmosphere, CO and CO_2 could react with H_2 to produce CO, CH_4, and H_2O, which decrease the CO conversion efficiency. It can be observed that the CO conversion and CO_2 selectivity are increased at temperatures above 250 °C. These results are obtained from the Boudouard reaction (1) which occurred due to the consumption of oxygen by hydrogen. CO is then dissociated to form carbon and CO_2.

3.3. Effect of Cu content

In this study, we initially chose 10 wt.% nominal Cu content to prepare catalysts for CO oxidation. The experimental results showed that the CNT-supported Cu catalysts exhibited good catalytic activity with highly dispersed Cu active sites. In order to study the effect of Cu content on CO oxidation and maximum metal loading weight on the nanoscaled material-CNT, we prepared different nominal Cu loading weights from 5 to 20 wt.%. The actual Cu content of catalysts was analyzed by ICP-MS. Fig. 6 shows the CO conversion on 4.0–18.1 wt.% (actual Cu content) Cu/CNT-I catalysts as a function of the reaction temperature. The inlet feed stream comprised 400 ppm CO and 6% O_2 in N_2 with a total space velocity of $1.56 \times 10^5\ h^{-1}$. In theory, the catalytic activity increases with the metal content on the catalyst. More active sites may increase the probability of reaction between the CO molecules and the Cu particles. Therefore, the CO conversion increases with the Cu content in the Cu/CNT-I catalysts, as shown in Fig. 6. However, the CO conversion efficiency did not increase, while the Cu content increased to 18 wt.%. The catalytic activity of catalysts with different Cu loading weights is in the following order: 13.4 wt.% > 18.1 wt.% = 7.5 wt.% > 4.0 wt.%. These results can be explained by TEM images, as shown in Fig. 7. The TEM images show the Cu/CNT-I catalysts with different loading weights, and illustrate that larger Cu particles with a low dispersion are aggregated on the CNT when the loading weight increases to 18.1 wt.%. Cu particles of size greater than 200 nm appeared at 18.1 wt.% actual Cu content catalyst, as shown in Fig. 7(d). Therefore, the optimum metal loading weight for the CNT catalyst prepared by the impregnation method is 13.4 wt.%.

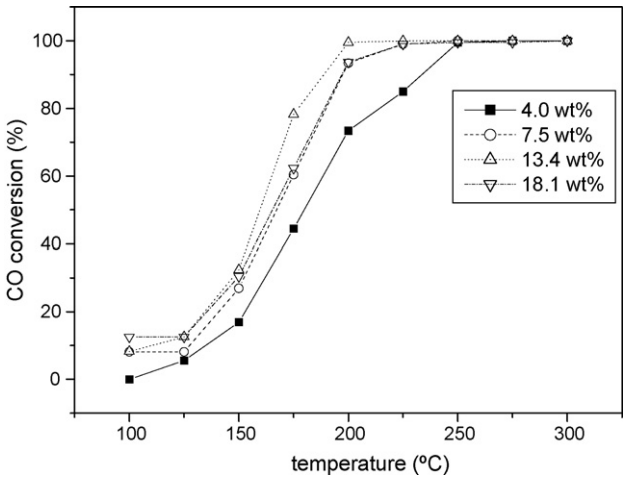

Fig. 6. CO conversion over Cu/CNT-I catalysts with 4.0–18.1 wt.% Cu as a function of the reaction temperature (feed composition: 400 ppm CO, SV = $1.56 \times 10^5\ h^{-1}$, and 6% O_2 in N_2).

3.4. Effect of CNTs with different diameters

It is well known that CNTs are available with various diameters. In this study, we chose a 20–40 nm CNT as a support to prepare a catalyst by impregnation and polyol processes (Fig. 2). In this section, we chose 10–20 nm and 60–100 nm CNTs as supports to prepare Cu/CNT-I catalysts for CO oxidation. The actual Cu content on the catalyst was chosen as 7.5 wt.%. Fig. 8 shows the CO conversion over the Cu/CNT-I catalysts prepared with the 10–20 nm and 60–100 nm CNTs. By comparing Fig. 1 with Fig. 8, we observed that the 10–20 nm CNT-supported Cu catalyst shows the best catalytic activity for 33% CO conversion at 125 °C. The CO conversion activity of catalysts containing CNTs of different diameters is in the following order: 10–20 nm > 20–40 nm > 60–100 nm. In order to confirm the effect of CNT diameter on CO oxidation, FESEM image of 60–100 nm Cu/CNT-I and the test results of O_2–temperature-programmed oxidation (TPO) were shown in Figs. 8 and 9. The inlet feed stream comprised 6% O_2 in N_2 with a total space velocity of $1.56 \times 105\ h^{-1}$. The heating rate was operated at 10 °C min^{-1}. Fig. 9 indicates that 60–100 nm Cu/CNT reacts with O_2 at a relatively lower temperature of 380 °C, followed by 20–40 nm Cu/CNT (430 °C) and 10–20 nm CNT (460 °C). The TPO experiment results showed that catalysts prepared with smaller diameters may enhance the thermo stabilization of CNT-supported catalyst. This suggested that no good dispersion and bigger size of Cu particles were prepared with the large diameters of CNT (as shown in Fig. 8). Rather, the large amount

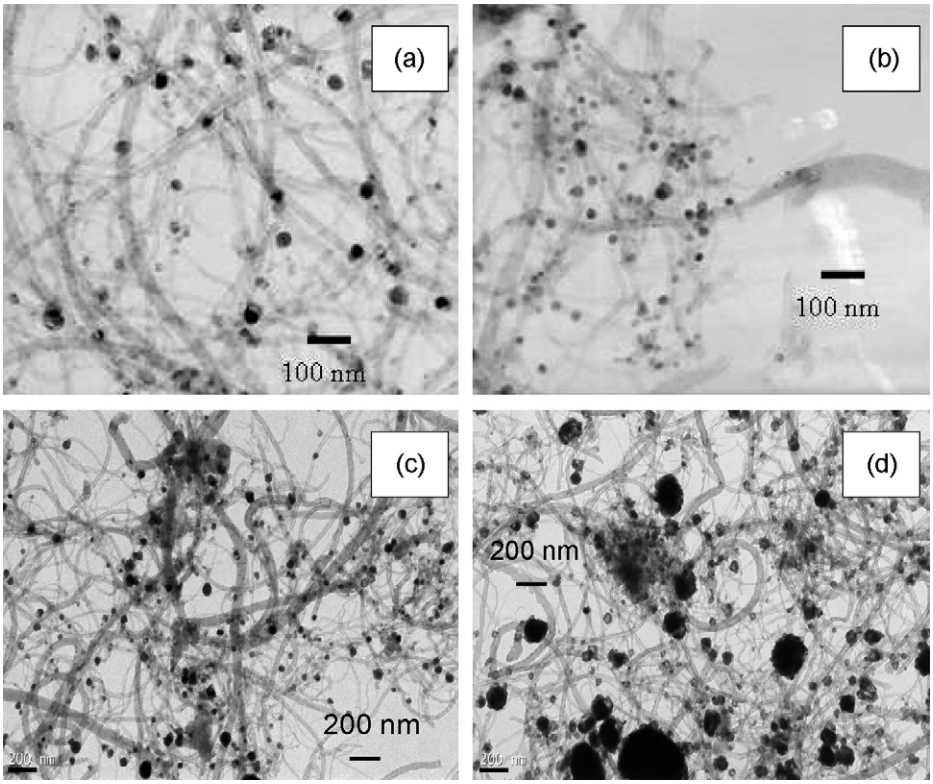

Fig. 7. TEM images showing the various copper loading weight of Cu/CNT-I: (a) 4.0 wt. %, (b) 7.5 wt. %, (c) 13.4 wt.%, (d) 18.1 wt.%.

of O_2 was taken by aggregated Cu particles at low temperature in the TPO test. In contrast, a good dispersion and smaller size of Cu particles were prepared with the smaller diameters of CNT. Consequently, the efficiency of O_2 removal was not obvious when reaction temperature was below 460 °C. From the point of catalytic oxidation, the oxygen may be consumed during the CO catalytic oxidation, producing CO_2 and heat energy. When O_2-Cu-CNT reaction was excited, in the case of O_2 and 60–40 nm Cu/CNT reaction, the exothermic reaction released a large amount of heat, which burned off the CNT support and decreased the catalytic activity.

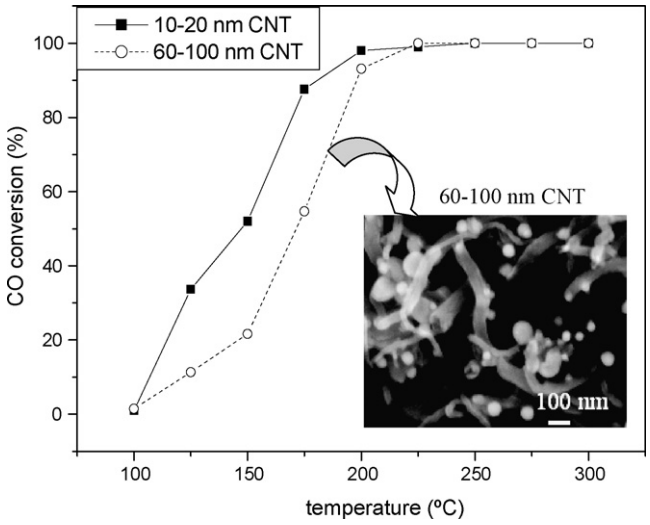

Fig. 8. CO conversion over Cu/CNT-I catalysts prepared with different diameter CNTs as a function of the reaction temperature: (■) 10–20 nm CNT and (○) 60–100 nm CNT (feed composition: 400 ppm CO, SV = 1.56×10^5 h^{-1}, and 6% O_2 in N_2).

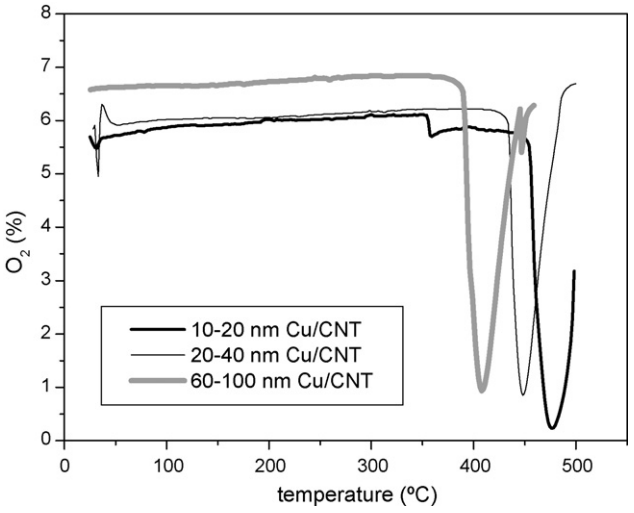

Fig. 9. O_2–TPO patterns over Cu/CNT catalysts with different diameters of CNTs.

When O_2-Cu-CNT reaction was not significant, the CNT support of catalyst would not burn off over the smaller diameter of CNT catalyst, resulting in good performance of CO conversion.

This suggests that CNTs with smaller diameters may be potential materials for increasing catalyst preparation efficiency, such as dispersion and crystalline size of the active phase, in order to enhance the performance of the catalytic reaction.

4. Conclusion

The objective of this work is to study the effect of catalyst preparation efficiency using the impregnation method and polyol process

with CNTs as catalyst supports. The effects of oxygen, hydrogen, metal loading weight, size of CNT, and catalyst preparation method on the CO conversion were also studied for CO conversion over CNT-supported catalysts.

A comparison of the impregnation method with the polyol process showed that the impregnation method is relatively simple for the fabrication of CNT-supported nanoscale Cu catalysts, whereas the polyol process showed no significant modification in the preparation of CNT-supported catalysts. The low activation energies of Cu/CNT-I and Cu/CNT-P were 57.47 and 77.45 kJ mol^{-1}, respectively. The experimental observations of the CO conversion in the H_2-rich atmosphere can be separated into the following three reaction zones depending on the temperature: (1) $CO + 1/2O_2 \rightarrow CO_2$ (<225 °C); (2) $H_2 + 1/2O_2 \rightarrow H_2O$, $CO_2 + H_2 \rightarrow CO + H_2O$, which were added into the reaction (>225 °C); and (3) $2CO \rightarrow C + CO_2$ was also observed in addition to the previous reactions (>250 °C).

In addition, the CO conversion is enhanced by increasing the Cu content on the CNT support with impregnation. The experimental results indicate that the optimum metal loading weight on the CNT for CO oxidation is 13.4 wt.%. Moreover, the catalytic activity of the Cu/CNT-I catalyst increases when CNTs with smaller diameters (10–20 nm) are chosen as supports for catalyst preparation.

References

[1] M.J. Illán-Gómez, A. Linares-Solano, L.R. Radovic, C. Salinas-Martínez de Lecea, NO reduction by activated carbons. 3: Some influence of catalyst loading on the catalytic effect of potassium, Energy Fuels 9 (1995) 104–111.

[2] C.Y. Lu, M.Y. Wey, The simultaneous removal of VOC and NO by activated carbon impregnated with transition metal catalysts in combustion flue gas, Fuel Process. Technol. 88 (2007) 557–567.

[3] J.B. Wang, W.H. Shih, T.J. Huang, Study of Sm_2O_3-doped CeO_2/Al_2O_3-supported copper catalyst of CO oxidation, Appl. Catal. A Gen. 203 (2000) 191–199.

[4] G. Avgouropoulos, T. Ioannides, C.H. Papadopoulou, J. Batista, S. Hocevar, A comparative study of Pt/γ-Al_2O_3, Au/α-Fe_2O_3 and CuO–CeO_2 catalysts for the selective oxidation of carbon monoxide in excess hydrogen, Catal. Today 75 (2002) 157–167.

[5] J.W. Park, J.H. Jeong, W.L. Yoon, H. Jung, H.T. Lee, D.K. Lee, Y.K. Park, Y.W. Rhee, Activity and characterization of the Co-promoted CuO–CeO_2/γ–Al_2O_3 catalyst for the selective oxidation of CO in excess hydrogen, Appl. Catal. A Gen. 274 (2004) 25–32.

[6] G. Che, B.B. Lakshmi, E.R. Fisher, R.M. Charles, Carbon nanotubule membranes for electrochemical energy storage and production, Nature 393 (1998) 346–349.

[7] S. Iijima, Helical microtubules of graphitic carbon, Nature 354 (1991) 56–58.

[8] H. Igarashi, H. Uchida, M. Suzuki, Y. Sasaki, M. Watanabe, Removal of carbon monoxide from hydrogen-rich fuels by selective oxidation over platinum catalyst supported on zeolite, Appl. Catal. A Gen. 159 (1997) 159–166.

[9] J. Garcia, H.T. Gomes, P. Serp, P. Kalck, J.L. Figueiredo, J.L. Faria, Platinum catalysts supported on MWNT for catalytic wet air oxidation of nitrogen containing compounds, Catal. Today 102-103 (2005) 101–109.

[10] G. Girishkumar, K. Vinodgopal, P.V. Kamat, Carbon nanostructures in portable fuel cells: Single-walled carbon nanotube electrodes for methanol oxidation and oxygen reduction, J. Phys. Chem. B 108 (2004) 19960–19966.

[11] C.Y. Lu, M.Y. Wey, The performance of CNT as support impregnated with non-noble metal for CO oxidation at low temperature, Fuel 86 (2007) 1153–1161.

[12] C.Y. Lu, M.Y. Wey, L.I. Chen, Application of polyol process to prepare AC supported nanocatalyst for VOC oxidation, Appl. Catal. A Gen. 325 (2007) 163–174.

[13] G. Carotenuto, Synthesis and characterization of poly(*N*-vinylpyrrolidone) filled by monodispersed silver clusters with controlled size, Appl. Organomet. Chem. 15 (2001) 344–351.

[14] D.H. Krinsley, K. Pye, S. Boggs, N.K. Tovey, Backscattered Scanning Electron Microscopy and Image Analysis of Sediments and Sedimentary Rocks, Cambridge University Press, 2005.

[15] J.W. Moore, R.G. Pearson, Kinetics and Mechanism, third ed., Wiley, New York, 1981.

[16] M.H. Khedr, K.S. Abdel Halim, M.I. Nasr, A.M. EI-Mansy, Effect of temperature on the catalytic oxidation of CO over nano-sized iron oxide, Mater. Sci. Eng. A Struct. Mater. Prop. Microstruct. Process. 430 (2006) 40–45.

[17] P. Mars, D.W. Van Krevelen, Oxidations carried out by means of vanadium oxide catalysts, Chem. Eng. Sci. 3 (1954) 41–59.

[18] P. Li, D.E. Miser, S. Rabiei, R.T. Yadav, M.R. Hajaligol, The removal of carbon monoxide by iron oxide nanoparticles, Appl. Catal. B Environ. 43 (2003) 151–162.